Sciknow Publications Ltd.
Research and Application of Material
©Attribution 3.0 Unported (CC BY 3.0)
RAM 2013, 1(1): 6-11
DOI: 10.12966/ram.05.02.2013

Analytical Expression for the Imaginary Part of the Dielectric Constant of Microcrystalline Silicon

C. Summonte, M. Allegrezza, M. Canino, M Bellettato and A. Desalvo

Consiglio Nazionale delle Ricerche, Istituto per la microelettronica e i microsistemi (CNR- IMM), via Gobetti 101 – 40129 Bologna, Italy

*Corresponding author (Email: caterina.summonte@cnr.it)

Abstract – An analytical function for the imaginary part of the dielectic constant of microcrystalline silicon is proposed. The function consists of a sum of Lorentz oscillators with Gaussian broadening, and is based on literature data. The real part is numerically obtained by Kramers-Kronig integration. The physical significance of the results is discussed. It is shown that the choice of the minimization procedure may affect the spectral region (low or high absorption) where the accuracy of the fit is optimized. The impact on computed Transmittance data shows the limits of acceptability for the errors in the fit.

Keywords - Microcrystalline Silicon, Dielectric Function, Optical Properties

1. Introduction

The dielectric constant of fine grained (FG) microcrystalline silicon was published by Jellison and coworkers in 1993 [1]. Since then, such function was applied to the analysis of silicon thin films in hundreds of publications and it is worldwide applied to a variety of topics, such as thin film and heterojunction solar cells, [2,3], the amorphous to crystalline transition [4], silicon nanowires [5], cells for automotive [6], ferroelectrics [7], imaging ellipsometry [8], silicon-carbon alloys [9], and many others. The function is available in a numerical form [10].

More recently, silicon nanocrystals have attracted interest because of quantum confinement inherent in their low dimensions [11,12]. The property is considered promising in photovoltaics [13-15] and in general in electronic applications of nanostructured materials [16-19].

The optical properties of nanocrystalline silicon are presently subject of intense investigation [20-29]. It would be of fundamental interest if the optical properties of nanocrystalline silicon could be related to their microcrystalline counterpart, by comparing physically significant analytical parameter, such as the frequency of the involved oscillators, as this comparison could in fact supply insight into the physics of the material itself [30,31]. For this reason, we focussed our attention on the derivation of an analytical expression of the dielectric constant of microcrsytalline silicon, based on the numerical data available in [10], that are based on the original Ref. [1].

A recent publication reports the analytical dielectric function of a set of samples that span from a-Si:H to μc-Si, obtained by PECVD under increasing hydrogen dilution (= parameter R) in Ref. [32]. In such reference, the sample that approaches at best the FG function [1] is obtained with R=50, and, compared with the FG function [1] has a lower E_2 peak amplitude (see below for details) and a larger tail absorption, which indicates the presence of residual a-Si:H [32, 33]. For higher R a drop in the E_1 peak is observed, that is attributed to free electrons associated to oxidation at grain boundaries [32]. For this reason the FG function is not an intermediate function of the set of samples of Ref. [32], and the analysis cannot be transfered to it. This is probably associated to the different preparation method, which, in case of Ref. [32] is focussed at the optimization of the technology of PECVD deposited thin film solar cells.

2. Calculations

All calculations reported in this paper were performed using the computer program GTB-fit [34] which is designed to fit numerical spectral forms of refractive index with several analytical forms, namely, a sum of Lorentz oscillators [35], the modified Tauc–Lorentz model proposed by Jellison and Modine [36], with possibility of including a Drude and a Sellmeier component. The fitting is based on the minimization of the χ^2 parameter or similar, and makes use of the minimization routine Minuit [37]. The program is also designed to simulate Reflectance and Transmittance (R&T) spectra, using the mathematics of the computer program Optical, based on generalized transfer matrix method [38]. The program is based on the open source platform Python. The numerical integration is performed by using the library

'SciPy', a Python extension for scientific calculations.

3. Method

Aim of this paper is to fit the dielectric function of fine-grained (FG) microcrystalline silicon of Ref. [1], where it is indicated as *p*-Si:ud, also available in [10] in tabular form. In the following, it will be referred to as FG.

The dielectric constant of solids can often be represented by a sum of analytical functions, normally harmonic oscillators, that are characterized by amplitude, energy, and broadening. The different functions do not necessarily reflect the singularities in the density of states, as the macroscopic dielectric function can be regarded as an integration over ***k*** space, which gives rise to somewhat dispersed absorption bands, usually with sharper edge on the low energy side, corresponding to the direct band gap. The fitting functions are therefore normally chosen basing on best fit criteria.

The imaginary part of the harmonic oscillator never vanishes. As a consequence the harmonic oscillator model fails to describe the drop of absorption around and below the energy gap [39]. This is a well known problem which has been addressed by a number of researchers. Several alternatives have been proposed, in particular for the case of amorphous materials. One option is the Tauc-Lorentz model, that is based on the validity of constant momentum approximation of the matrix element, and was proposed by Jellison and Modine [36]. In such model, the contribution of a single Lorentz oscillator is multiplied by the Tauc joint density of states. The model was successively widely applied, mainly to amorphous materials, and further developed by many authors [30,40-41].

Another method to achieve independent control of the low absorption region is to replace the constant broadening of the Lorentz oscillator with a Gaussian-like energy dependent broadening function. This method, that is more suitable to describe complicated bands composed by a sum of oscillators, as is the case of crystalline materials or vibrational spectra, was originally introduced by Kim et al. in a very accurate but complex model [39], and was later applied to the simpler Lorentz oscillator model (G-L model in the following) [42,43]. The Gaussian broadening, through the lineshape parameter α, basically weakens the contribution of the oscillator for energies sufficiently apart from the oscillator energy, and allows accurate description of the imaginary part of the dielectric function. The main drawback of this model is that the real and imaginary parts of the complex dielectric function are no longer Kramers-Kronig transforms of each other, as also pointed out in Ref. [44]. To avoid matematically and physically incorrect results, the real part must be evaluated by KK numerical integration of the imaginary part [45].

In this work, we make use of this combined approach, in which the imaginary part of the dielectric constants is deconvoluted into a sum of G-L oscillators. The real part of the dielectric constant is obtained by numerical KK-integration of ε_2. This procedure is mandatory to obtain a good fit of the FG data.

The formulation used within this paper is the following:

$$\varepsilon_2(E) = \sum_i \frac{\left((A_i - 1)\cdot E_{0i}^{\;2}\right)\cdot \Gamma_{Bi} \cdot E}{\left(E_{0i}^2 - E^2\right)^2 + \left(\Gamma_{Bi}\cdot E\right)^2} \tag{1}$$

where A_i, E_i, Γ_i are the amplitude, energy, and broadening of oscillator *i*, and *E* is the photon energy. The energy dependent broadening parameter Γ_{Bi} is given by:

$$\Gamma_{Bi} = \Gamma_i \cdot e^{-\alpha_i \cdot \left(\frac{E - E_{0i}}{\Gamma_i}\right)^2} \tag{2}$$

where α_i is the lineshape parameter of oscillator *i*.

The real part was numerically obtained by KK transformation of ε_2:

$$\varepsilon_1(E) = 1 + \frac{2}{\pi} P \int_0^\infty \frac{\omega \cdot \varepsilon_2(\omega)}{\omega^2 - E^2} d\omega \tag{3}$$

where *P* is the Cauchy principal value of the integral.

Three different fitting procedures were attempted: minimization of χ^2 (eq. (4)):

$$\chi^2 = \sum_E \left(\frac{(\varepsilon_{J1}(E) - \varepsilon_{M1}(E))^2}{\sigma^2} + \frac{(\varepsilon_{J2}(E) - \varepsilon_{M2}(E))^2}{\sigma^2} \right) \tag{4}$$

using four oscillators, and minimization of the Pearson χ^2 function (eq. (5)),

$$P = \sum_E \left(\frac{(\varepsilon_{J1}(E) - \varepsilon_{M1}(E))^2}{(\varepsilon_{J1}(E))} + \frac{(\varepsilon_{J2}(E) - \varepsilon_{M2}(E))^2}{(\varepsilon_{J2}(E))} \right) \tag{5}$$

using either three or four oscillators. In the above equations, σ is the standard deviation, and ε_M and ε_J are the computed and FG values of the dielectric constant respectively. In all cases, the broadening parameter α was limited to 2, which is larger than the proposed maximum value 0.3 [43]. The value was chosen because it allows a very efficient elimination of the tails, still resulting in an absorption band reasonably similar to a Gaussian.

In the following, the different procedures will be referred to as X4, P3, and P4 respectively. In case X4, in the absence of information on standard deviation of original data, the arbitrary value 0.1 was chosen, that, being constant, does not affect the result of the minimization. As we will see, the choice of the minimization function brings about substantial differences. Results obtained using two oscillators, as well as using constant-broadening Lorentz oscillators, supplied a poor fit and are not reported.

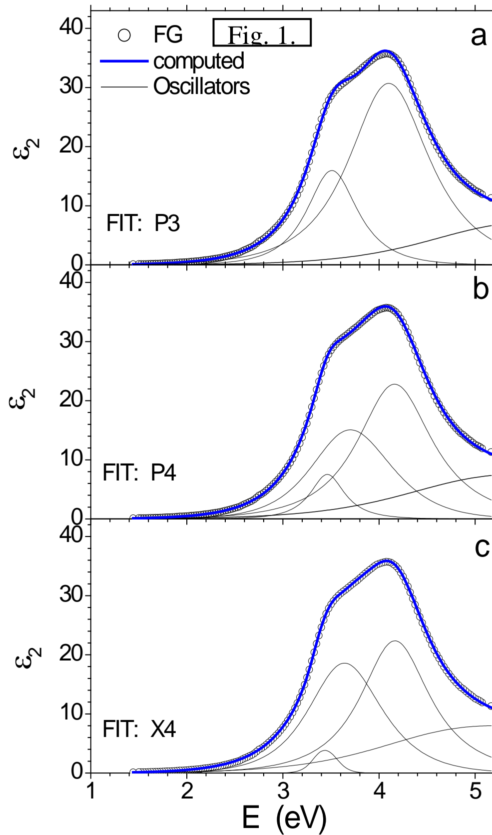

Fig. 1. (color online) a,b,c: result of the simulation. Symbols: FG data. Bold (blue) line: ε2 computed P3 (a) P4(b) or X4 (c) minimization procedure. The deconvolution into separate oscillators is also plotted in each figure (thin lines).

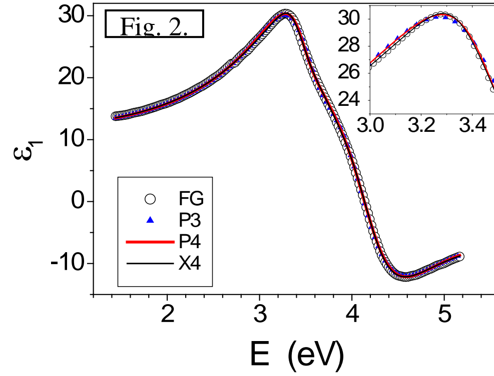

Fig. 2. (color online) – Real part of the dielectric constant of FG data, and data obtained from P3, P4, and X4 fitting procedure.

Table 1. Fine-grained microcrystalline silicon: Amplitude, energy, broadening, and lineshape parameter of oscillators for ftting models P3, P4, X4. The parameters are valid in the spectral region 1.2 to 5.5 eV.

Oscillators		A	E eV	Γ eV	α
P3	1	3.7982	3.5246	0.6188	0.3113
	2	8.3392	4.1334	0.9917	0.3163
	3	4.6918	5.9392	3.1062	1.5386
P4	1	1.9130	3.4688	0.4204	0.2038
	2	4.9670	3.7414	0.9896	0.6640
	3	5.9781	4.1891	0.9177	0.2571
	4	5.2268	5.8243	3.3575	1.6018
X4	1	1.3376	3.4414	0.3031	1.2711
	2	5.5329	3.6724	0.8993	0.5341
	3	5.5297	4.1890	0.8507	0.2459
	4	5.9170	5.6635	3.6377	1.9999

4. Results

Fig.1 reports the FG ε_2 data, and the results of the fitting procedures. The deconvolution into separate oscillators is also plotted. The ε_1 data obtained from Kramers-Kronig numerical integration (Eq (3)) are reported in Fig. 2. The figures shows a good fit in all cases. The parameters of all oscillators are reported in Table 1.In all cases, an oscillator in the UV, with energy out of the data spectral range, is needed, to account for the asymetrical shape of the absorption band, and can be regarded as a reminescence of the E_1' critical point in c-Si [46]. Different parameters for such oscillator are likely to be found if spectral data that expand further in the UV are available.

The 3-5 eV absorption band can be succesfully simulated with two additional oscillators (case P3) for a total of 12 parameters. The oscillator at lower energy reflects the energy position of the E_0' and E_1 transitions, both smeared out [47] similarly to what occurs in partially amorphized c-Si [48], or c-Si at high temperature [46]. The energy of this oscillator is somewhat higher than that previously used as fixed parameter in the literature (3.36 eV in the analysis of Ref. [32]), probably as a consequence of the symmetry of the oscillators in our case, and compares with 3.38 eV found for c-Si [49]. The oscillator at higher energy reflects the E_2 critical point, moved to a somewhat lower energy with re-

spect to the c-Si case [47]. The feature is attracting, because the physical significance of the model is maintained. Using four oscillators (case P4, 16 parameters) results in a decrease of χ^2 from 1.1E-2 to 9.3E-5. In this case, the $E_o' E_1$ band is resolved into two oscillators, however, it is probably speculative to invoke a direct quantitative correlation with transitions at the critical points. The amplitude of the oscillator at E_2 is reduced. The X4 case supplies an equally good fit, however differently distributed over the spectrum. To make this point clear, an enlargement of ε_2 in the low (a) and high (b) absorption regions is reported in Fig. 3. The P4 case minimizes not the sum of the squared residuals, but the squared residuals divided by the expected values. In this way, more weight is given to the low absorption region. In fact, Fig. 3 shows that a better fit is obtained using P4 in the 2-2.5 eV region, whereas X4 gives the best fit in the high absorption region.

The result is also visible in Fig. 4, where all errors and relative errors are reported. A spike in $\delta\varepsilon_1/\varepsilon_1$ occurs at the energy at which ε_1 vanishes. Smaller errors are detected for the P4 rather than the P3 case, which justifies the choice of four oscillators (16 parameters).

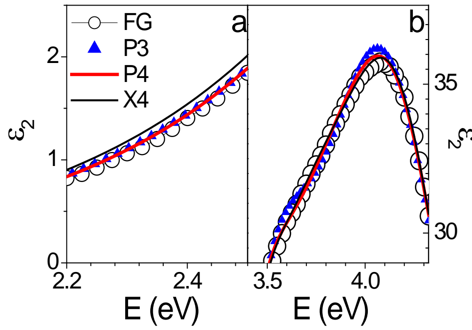

Fig. 3. (color online)– Enlargement of the result of the fitting procedures on ε_2, on the low (a) and high (b) absorption region.

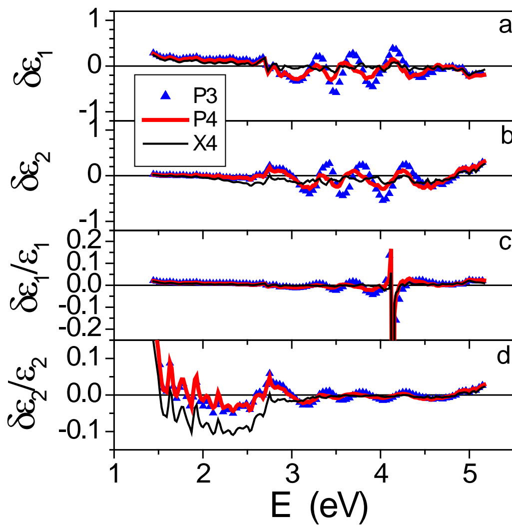

Fig. 4. Errors and percent errors in the dielectric constant determined using three (symbols) and four (line) oscillators.

Case X4 shows smaller errors compared to P4, however, a relative error as high as 10% is detected in the low absorption region (2 to 2.6 eV, see Fig. 4d. How this affects the simulation of experimental spectra will be illustrated in the next section.

5. Application to elaboration of experimentally accessible data

To verify the impact of the different cases on simulation of experimental data, we computed the Reflectance and Transmittance spectra (R&T) of 120 nm microcrystalline silicon on quartz, using the FG $\varepsilon_1,\varepsilon_2$ data, and the $\varepsilon_1,\varepsilon_2$ data obtained from the fitting procedures. We chose the R&T technique because it is particularly sensitive to the medium-low (= around band-gap) absorption. The spectra are computed using the program Optical [38]. The dielectric function of quartz was taken from Ref. [50]. In Fig.5, three regions can be identified (the energy extremes are indicative, as they depend on thickness): the region of transparency (E<2 eV) where T and R are symmetrical with respect to 50%; the high absorption (E>3 eV), where T=0; and a low absorption region in between, where T is partially limited by absorption, that is, 1-R-T is larger than the sum of the R and T experimental errors. In the high absorption region, the two R peaks are related to the ε_2 critical points, whereas for lower absorption an interference pattern is visible, due to multiple reflections at the film-substrate interface.

Fig 5 shows that the overall R&T spectrum is well reproduced, however, the local transmittance maximum at 2.34 eV photon energy is underestimated in case X4, see the enlargement in the inset. Specifically, (i.e. for thickness = 120 nm), a $\delta\varepsilon_2 = 0.13$ (Fig.3), corresponding to $\delta\varepsilon_2/\varepsilon_2= 10\%$ (Fig. 4(d)), reflects in a $\delta T = 0.02$ (Fig. 5, inset), which is at least a factor four larger than the best achievable experimental accuracy. In fact, in the low absorption region, T is particularly sensitive to the imaginary part of the dielectric function [40]. On the one hand, this allows to accurately detect moderate absorption, which is of interest in specific applications as for instance thin film solar cells. On the other hand, if $\varepsilon_1,\varepsilon_2$ spectra of all involved materials are not known to the needed accuracy, remarkable errors can arise in the determination of volume fractions when the R&T data are elaborated in order to detect the various components of an Effective Medium [51,52] material. An example is the determination of the crystallized fraction of annealed silicon thin films [15,53].

We stress the importance of accuracy of ε_2 spectra in the low-absorption region when determined for istance by ellipsometry, which is a technique that is known to perform at best in the high absorption region [32,40]. This is particularly true if ellipsometric data are elaborated by fitting to a model of the dielectric function [31]. The choice for the dielectic function is likely to affect the results at the long wavelength side of the spectral range, where the small

values of ε_2 may well risk of being underweighted in the overall fit, thus leading to a large relative deviation. This can have consequences in practical applications. We make the example of the top cell of a tandem photovoltaic device, that is designed to absorb the solar radiation in the range 1.7 to 3 eV. A candidate material for such a device are silicon nanodots [13,14], that, because of quantum confinement, are expected to have blue shifted absorption with respect to that reported in Fig. 1 [31]. It is evident by inspection of Figs. 1 and 5 that an error in the determination of the low absorption tail may lead to a dramatic error in the determination of the needed absorber thickness in actual photovoltaic devices [54].

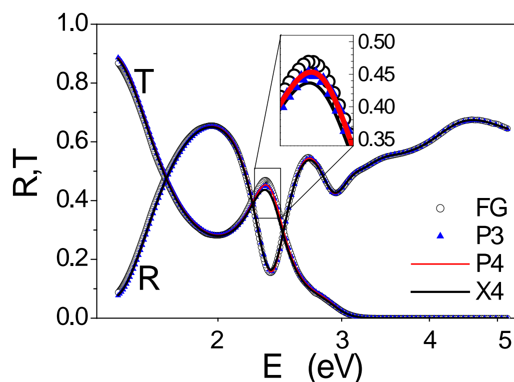

Fig. 5. R&T spectra of 120 nm fine grained microcrystalline silicon on quartz, computed using the FG, P3, P4, and X4 dielectric constants. The region of interest is enlarged in the inset.

Finally, one may argue that, if precise values of low absorption are to be determined, the fit could be done directly on R&T. However, as the transmittance is zero at short wavelengths, this reduces the useful energy spectrum for the minimization. The spectrum can be extended in the blue by decreasing the thickness, but this directly reduces the sensitivity of T on absorption.

6. Summary and Conclusions

In summary, we present an analytical description of the imaginary part of the dielectric function of fine grained microcrystalline silicon [1], obtained using either three or four Oscillators with Gaussian broadening. Slightly different results are obtained using different fitting procedures. The X4-four oscillator model gives substantial agreement to the original data in the high absorption region, whereas superior performance in the moderate absorption region is obtained using the P4 model. The impact of the obtained differences, and, more in general, of the accuracy of ε_2 at long wavelengths, on the elaboration of experimentally accessible spectrophotometric data, is discussed. Only moderately reduced accuracy is obtained using the P3-three oscillator model, with the advantage of a lesser number of parameters (twelve), yet retaining their physical significance. This is probably the best starting point for the evaluation of the experimental spectra of advanced silicon based nanostructured materials, as is the case of silicon nanocrystals.

Acknowledgments

The research leading to these results has received funding from the European Community's FP7 (FP7/2007-2013) under grant agreement n°. 245977 under the project title NASCEnT

References

[1] G.E. Jellison, M.F. Chisholm and S.M. Gorbatkin, Appl. Phys. Lett. 62 (1993) 3348
[2] M. Moreno, R.Boubekri, P.Roca i Cabarrocas, Solar Energy Materials and Solar Cells 100 (2012) 16
[3] J. Plà, E. Centurioni, C. Summonte, R. Rizzoli, A. Migliori, A. Desalvo, F. Zignani, Thin Solid Films 405 (2002), 248
[4] A. Hadjadj, N. Pham, P. Roca i Cabarrocas, O. Jbara, and G. Djellouli, J. Appl. Phys. 107 (2010) 083509
[5] Z.Y. Guo, J.Y. Jung, K.Y. Zhou, Y.J. Xiao, S.W. Jee, S.A. Moiz, J.H. Lee, in Next Generation (Nano) Photonic and Cell Technologies For Solar Energy Conversion, L. Tsakalakos (Ed.), Proc. SPIE, Vol. 7772, 2010, DOI: 10.1117/12.860397
[6] Z.T. Kuznicki, P. Meyrueis, in Photonics In The Transportation Industry: Auto To Aerospace III, Proc. SPIE Vol. 7675, 2010, DOI: 10.1117/12.852687
[7] Y.M. Chen, R.J. Zhang, Y.X. Zheng, P.H. Mao, W.J. Lu, L.Y. Chen, J. Korean Physical Society 53 (2008) 2299
[8] A. J. Choi, T. H. Ghong, and Y. D. Kim, J. H. Oh J. Jang, J. Appl. Phys. 100 (2006) 113529
[9] M. Losurdo, M. Giangregorio, P. Capezzuto, G. Bruno, F. Giorgis, J. Appl. Phys. 97 (2005) 103504
[10] http://refractiveindex.info/?group=CRYSTALS&material=poly-Si
[11] M. Zacharias, J. Heitmann, R. Scholz, U. Kahler, M. Schmidt, J. Bläsing, Applied Physics Letters 80 (2002) 661.
[12] A. M. Hartel, S. Gutsch, D. Hiller, and M. Zacharias, Phys. Rev. B 85 (2012) 165306
[13] M.A. Green, Third Generation Photovoltaics – Advanced Solar Energy Conversion, Springer, Berlin, Heidelberg, New York, 2003.
[14] S. Janz, P. Löper, M. Schnabel, S. Janz, et al., Mater. Sci. Eng. B (2012), in press. Available at: http://dx.doi.org/10.1016/j.mseb.2012.10.018
[15] C. Summonte, M. Canino, M. Allegrezza, M. Bellettato, A. Desalvo, S. Mirabella, A. Terrasi, Proc. 26th European Photovoltaic Solar Energy Conference, Sept. 5-9 2011, Hamburg (D), p.361
[16] D. Nesheva, N. Nedev, E. Manolov, I. Bineva, H. Hofmeister, J. of Physics and Chemistry of Solids 68 (2007) 725
[17] R. Lechner, A.R. Stegner, R.N. Pereira, R. Dietmueller, M.S. Brandt, A. Ebbers, M. Trocha, H. Wiggers, M. Stutzmann, J. Appl. Phys 104 (2008) 053701
[18] Y.C. Lien, J.M. Shieh, W.H. Huang, C.H. Tu, C. Wang, C.H. Shen, B.T. Dai, C.L. Pan, C. Hu, F.L. Yang, Appl. Phys. Lett. 100 (2012) 143501
[19] D. Nesheva, N. Nedev, M. Curiel, I. Bineva, B. Valdez and E. Manolov (2012), in Quantum Dots - A Variety of New Applications, Dr. Ameenah Al-Ahmadi (Ed.), ISBN: 978-953-51-0483-4,

InTech, Available from: http://www.intechopen.com/books/quantum-dots-a-variety-of-new-applications
[20] S. Charvet, R. Madelon, R. Rizk, Solid-State Electronics 45 (2001) 1505
[21] D. Amans, S. Callard, A. Gagnaire, J. Joseph, G. Ledoux, F. Huisken, J. Appl. Phys. 93 (2003) 4173
[22] L. Ding, T. P. Chen, Y. Liu, C. Y. Ng, and S. Fung, Phys. Rev. B 72 (2005) 125419
[23] J.A. Moreno, B. Garrido, P. Pellegrino, C. Garcia, J. Arbiol, J.R. Morante, P. Marie, F.Gourbilleau, R. Rizk, J. Appl. Phys. 98 (2005) 013523
[24] C. Bulutay, Phys. Rev. B 76 (2007) 205321
[25] I. Stenger, B. Gallas, L. Siozade, C.-C. Kao, S. Chenot, S. Fisson, G. Vuye, J. Rivory, J. Appl. Phys 103 (2008) 114303
[26] M. Losurdo, M.Bergmair, G. Bruno, D. Cattelan, C. Cobet, A. de Martino, K. Fleischer, Z. Dohcevic-Mitrovic, N. Esser, M. Galliet, R. Gajic, D.an Hemzal, K. Hingerl, J. Humlicek, R. Ossikovski, Z. V. Popovic, O. Saxl, J. Nanopart Res 11 (2009) 1521
[27] C. Summonte, E. Centurioni, A. Desalvo, M. Canino, S. Mirabella, R. Agosta, F. Simone, A. Terrasi, M. A. Di Stefano, S. Di Marco, S. Ravesi, and S. Lombardo, Proc. 26th European Photovoltaic Solar Energy Conference, Sept. 21-25 2006, Hamburg (D), p.317
[28] M. I. Alonso, I. C. Marcus, M. Garriga, and A. R. Goñi, Phys. Rev. B 82 (2010) 045302
[29] S. Ossicini, M. Amato, R. Guerra, M. Palummo, O. Pulci, Nanoscale Res. Lett. 5 (2010) 1637
[30] H. Chen, W.Z. Shen, Eur. Phys. J.B 43 (2005) 503
[31] J. Budai, I. Hanyecz, E. Szilágyi, Z. Tóth, Thin Solid Films 519 (2011) 2985
[32] T. Yuguchi, Y. Kanie, N. Matsuki, H. Fujiwara, J. Appl. Phys. 111 (2012) 083509
[33] S. Boultadakis, S. Logothetidis, S. Ves, J. Kircher, J. Appl. Phys. 73 (1993) 914.
[34] [34] C. Summonte, F. Gaspari, M. allegrezza, M. Canino. M. Bellettato, A. Desalvo, submitted. See also: http://www.bo.imm.cnr.it/users/allegrezza/minuit/
[35] J. Leng, J. Opsal, H. Chu, M. Senko, D.E. Aspnes, J. Vac. Sci. Technol. A16 (1998) 1654
[36] G.E. Jellison, F.A. Modine, Applied Physics Letters 69 (1996) 371–373 and Erratum in Appl. Phys. Lett 69 (1996) 2137
[37] http://code.google.com/p/pyminuit/
[38] E. Centurioni, Applied Optics 44 (2005) 7532–7539; see also: http://www.bo.imm.cnr.it/users/centurioni/optical.html
[39] C.C. Kim, J.W. Garland, H. Abad, P.M. Raccah, Phys. Rev. B 45 (1992) 11749
[40] A.S. Ferlauto, G.M. Ferreira, J.M. Pearce, C.R. Wronski, R.W. Collins, X. Deng, G. Ganguly, J. Appl. Phys 92 (2002) 2424
[41] M. Foldyna, K. Postava, J. Bouchala, J. Pištora, T. Yamaguchi, Proc. SPIE 5445 (2004) 301
[42] A. B. Djurišić, E. H. Li, Applied Optics 37 (1998) 5291
[43] A.D. Rakić, M. L. Majewski, J. Appl. Phys. 80 (1996) 5909
[44] M. Muñoz, Fred H Pollak, Todd Holden, Semicond. Sci. Technol. 16 (2001) 281
[45] M. Schubert, J. A. Woollam, G. Leibiger, B. Rheinländer, I. Pietzonka, T. Sass, V. Gottschalch, J. Appl. Phys. 86 (1999) 2025
[46] P. Lautenschlager, M. Garriga, L. Viña, M. Cardona, Phys. Rev. B36 (1987) 4821
[47] G.E. Jellison, in Handbook of Silicon Semicon. Metrology, Ed. A.C. Diebold, New York, 2001
[48] P. K. Giri, S. Tripurasundari, G. Raghavan, B. K. Panigrahi, P. Magudapathy, K. G. M. Nair, and A. K. Tyagi, J. Appl. Phys 90 (2001) 659
[49] J. Leng, J. Opsal, H. Chu, M. Senko, D.E. Aspnes, Thin Solid Films 313-314 (1998) 132
[50] E.D. Palik (Ed.), Handbook of Optical Constants of Solids, Academic Press, Inc., Orlando, FL, 1985
[51] D.A.G. Bruggeman, Ann. Phys. (Leipzig) 24 (1935) 636
[52] H. Fujiwara, J. Koh, P. I. Rovira, R. W. Collins, Phys. Rev. B 61 (2000) 10832
[53] C. Summonte, E. Centurioni, M. Canino, M. Allegrezza, A. Desalvo, A. Terrasi, S. Mirabella, S. Di Marco, M.A. Di Stefano, M. Miritello, R. Lo Savio, R. Agosta, Phys. Status Solidi C8 (2011) 996
[54] C. Summonte, E. Centurioni, A. Desalvo, M. Canino, S. Mirabella, R. Agosta, F. Simone, A. Terrasi, M. A. Di Stefano, S. Di Marco, S. Ravesi, and S. Lombardo, 24th EPVSEC, 21-25 Sept 2009, Hamburg (D), p.317